Available online at www.sciencedirect.com
ScienceDirect
Journal of Power Sources 175 (2008) 657–663
JOURNAL OF POWER SOURCES
www.elsevier.com/locate/jpowsour

Anodic deposition of porous RuO_2 on stainless steel for supercapacitor studies at high current densities

Sujit Kumar Mondal, N. Munichandraiah *

Department of Inorganic and Physical Chemistry, Indian Institute of Science, Bangalore 560012, India

Received 2 June 2007; received in revised form 14 August 2007; accepted 22 August 2007
Available online 7 September 2007

Abstract

Ruthenium dioxide is deposited on stainless steel (SS) substrate by galvanostatic oxidation of Ru^{3+}. At high current densities employed for this purpose, there is oxidation of water to oxygen, which occurs in parallel with Ru^{3+} oxidation. The oxygen evolution consumes a major portion of the charge. The oxygen evolution generates a high porosity to RuO_2 films, which is evident from scanning electron microscopy studies. RuO_2 is identified by X-ray photoelectron spectroscopy. Cyclic voltammetry and galvanostatic charge–discharge cycling studies indicate that RuO_2/SS electrodes possess good capacitance properties. Specific capacitance of 276 F g^{-1} is obtained at current densities as high as 20 mA cm^{-2} (13.33 A g^{-1}). Porous nature of RuO_2 facilitates passing of high currents during charge–discharge cycling. RuO_2/SS electrodes are thus useful for high power supercapacitor applications.

Keywords: Porous RuO_2; Anodic deposition; Stainless steel substrate; Supercapacitor; Cyclic voltammetry; Charge–discharge cycling

1. Introduction

Ruthenium dioxide has been studied as a promising electrode material for supercapacitor studies [1–7]. Several approaches have been reported for preparation of RuO_2 [2–14]. RuO_2 is an oxidation product on surface of Ru metal by subjecting the metal to cyclic voltammetry in H_2SO_4 electrolytes. RuO_2 grows as a thick film by repeated cycling [4]. RuO_2 films are also prepared by painting a solution of $RuCl_3$ on a metallic substrate such as Ti and subsequently heating [2,3]. Chemical oxidation of $RuCl_3$ to produce RuO_2 powder is another route [8–12]. For the purpose of electrochemical characterization, the powder of RuO_2 thus formed can be coated on a metallic current collecting substrate using a suitable binder. For the electrochemical deposition of RuO_2 from an aqueous solution of $RuCl_3$, both cathodic and anodic deposition methods have been employed [13]. Cathodic galvanostatic deposition of RuO_2 on Ni, Ti, Pt and Si foils is accomplished via hydrolysis of $RuCl_3$ by electrochemically generated base [13]. By varying current density (10–70 mA cm^{-2}) and deposition time in 5 mM $RuCl_3$ aqueous solution, the quantity of the deposited material has been controlled. X-ray diffraction (XRD) studies have indicated that metallic Ru is also present in an amorphous phase of freshly prepared cathodic RuO_2 deposits. Although RuO_2 electrodeposited films have been characterized by various studies such as XRD, thermal analysis, scanning electron microscopy (SEM), etc. capacitance properties have not been studied [13]. Cathodic electrodeposition of RuO_2 thin films on Ti substrate has also been studied by Park et al. [14]. A specific capacitance value of 788 F g^{-1} has been obtained for a RuO_2/Ti electrode with RuO_2 loading level of 1.4 mg cm^{-2}. However, galvanostatic charge–discharge data have not been reported [14]. Hydrous RuO_2-coated Ti electrodes have been prepared by cyclic voltammetry in the potential range −0.2–1.0 V from an aqueous solution of $RuCl_3$ by Hu and Huang [15]. The electrodes have been subjected to charge–discharge cycling at a current density of 100 μA cm^{-2} and a specific capacitance of about 100 F g^{-1} has been obtained. In spite of the fact that several metal oxides such as MnO_2, PbO_2, etc. are prepared by anodic oxidation of the respective metal ions dissolved in an appropriate electrolyte, there are only a few reports on anodic synthesis of RuO_2 [16,17]. Anderson and Warren [16] have first reported the possibility of anodic deposition of RuO_2 on a Pt disk electrode at 0.9 V versus SCE in an aqueous solution of ben-

* Corresponding author. Tel.: +91 80 22933183; fax: +91 80 23600683.
E-mail address: muni@ipc.iisc.ernet.in (N. Munichandraiah).

0378-7753/$ – see front matter © 2007 Elsevier B.V. All rights reserved.
doi:10.1016/j.jpowsour.2007.08.104

zene ruthenium(II) complex at pH ∼ 5. The reversible behaviour of the electrodeposited RuO_2 has been demonstrated in 0.1 M $HClO_4$ solution. The films have slowly dissolved in aqueous electrolytes upon potential cycling. In a recent study, Hu et al. [17] have reported anodic deposition of $RuO_2{\cdot}xH_2O$ onto Ti substrate from a simple chloride precursor solution. The deposition of RuO_2 is catalyzed by acetate ion in the electrolyte. The specific capacitance of RuO_2 has been shown to increase by annealing at 150 °C.

Electrochemical deposition is a simple, one-step and cost-effective method for electrode preparation. The texture, surface morphology and uniformity of deposits can be controlled by adjusting the experimental variables such as potential, applied current density, temperature, concentrations, etc. Thus, the electrodeposited RuO_2 on a suitable current -collecting substrate is more advantageous than the electrodes prepared using RuO_2 powders. During the cathodic deposition of RuO_2, it has been found that co-deposition of metallic Ru also takes place [13]. The X-ray photoelectron spectroscopy (XPS) studies of RuO_2 deposited by potentiodynamic technique in $RuCl_3$ aqueous solution have indicated the presence of mixed hydroxyl ruthenium species at various oxidation states and also $RuCl_3$ [15]. Due to the coexistence of metallic Ru or $RuCl_3$, the specific capacitance values of RuO_2 are low. It is expected that the anodic deposition of RuO_2 would be free from the problem of coexistence of metallic Ru and also $RuCl_3$. In the present work, anodic deposition of RuO_2 on stainless steel (SS) substrate is carried out and the RuO_2/SS electrodes are characterized for capacitor studies. A common metal or alloy such as SS is anticipated to be cost-effective for practical applications. Interestingly, the anodically deposited RuO_2 films are found to possess high porosity due to simultaneous oxygen evolution during the RuO_2 deposition. The porous RuO_2/SS electrodes are found useful for passing high current densities (c.d.) during charge–discharge cycling of supercapacitor studies.

2. Experimental

Analytical grade chemicals were used without further purification. $RuCl_3{\cdot}xH_2O$ was purchased from Loba Chemicals. Double distilled water was used for preparation of all solutions. For anodic deposition of RuO_2, an aqueous solution of 0.01 M (or 0.1 M) $RuCl_3$ in 0.1 M HCl was prepared. A commercial SS of grade 304 was employed as the substrate for deposition of RuO_2. A sheet of SS (thickness: 0.2 mm) was subjected to sandblasting, which produced oxide-free surface with visually noticeable roughness. Strips (10 mm × 100 mm) of the sandblasted SS were sectioned out of the sheet, cleaned with detergent, etched in dil. HCl, washed with double distilled water, rinsed with acetone and dried under vacuum for several hours at ambient temperature. A glass cell of 50 ml capacity, which had provision to introduce SS working electrode, Pt auxiliary electrodes and a saturated calomel electrode (SCE) reference, was used for all electrochemical studies. About 20 ml of $RuCl_3$ solution was used as the electrolyte for deposition of RuO_2. The SS electrode of area 2 cm^2 at an end of the strip was exposed to the electrolyte, and rest of the strip was used as the current collector. The electrode was weighed before and after RuO_2 deposition. The mass of RuO_2 deposited on SS was about 1.5 mg cm^{-2}. Anodic deposition of RuO_2 was carried out galvanostatically at various current c.d. in the range of 15–35 mA cm^{-2}. Electrochemical characterization of RuO_2/SS electrodes was performed in 0.5 M H_2SO_4 solution in a three-electrode cell employing Pt auxiliary electrodes and a SCE reference electrodes. Potential values are reported against SCE.

A Sartorious electronic balance model CP2250D-OCE with 0.01 mg sensitivity was used for weighing the electrodes. Microstructure of the electrodeposited RuO_2 films of SS substrate were examined by FEI scanning electron microscope model Sirion and XPS spectra were recorded using VG Scientific spectrometer. For anodic deposition of RuO_2, cyclic voltammetry and galvanostatic charge–discharge cycling, Eco-chemie potentiostat/galvanostat model Autolab 20 or EG&G PARC potentiostat/galvanostat model Versastat were employed. All experiments were carried out at 221 ± °C.

3. Results and discussions

Oxidation of Ru^{3+} to RuO_2 can occur electrochemically in aqueous electrolytes according to reaction (1).

$$Ru^{3+} + 2H_2O \rightarrow RuO_2 + 4H^+ + e^- \quad (1)$$

As RuO_2 is insoluble in the electrolyte, it deposits on the anode.

Galvanostatic steady-state polarization data for a Pt electrode in an uniformly stirred 0.01 M $RuCl_3$ electrolyte were measured in the potential range 0.8–2.6 V. The Tafel plot is shown in Fig. 1. There is a fairly linear Tafel region between 1.0 and 1.2 V. This region corresponds to RuO_2 deposition (reaction (1)). The current–potential relationship follows the Butler–Volmer equation (Eq. (2)).

$$i = i_0 \exp\left[\frac{\beta F(E - E^\circ)}{RT}\right] \quad (2)$$

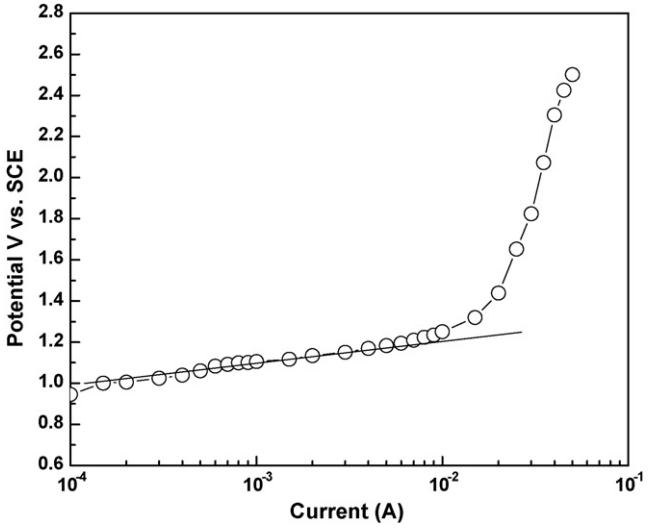

Fig. 1. Tafel polarization data for Pt in 0.01 M $RuCl_3$ + 0.1 M HCl electrolyte (area of the electrode = 0.6 cm^2).

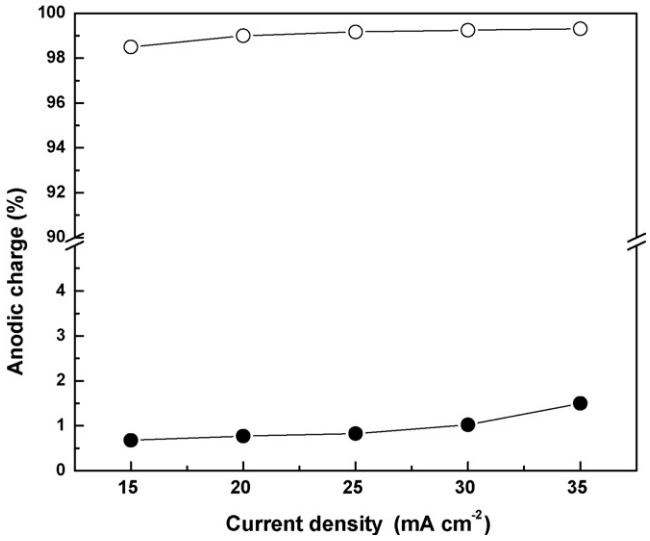

Fig. 2. Anodic charge in percent consumed for oxygen evolution (◯) and for RuO_2 deposition (●) against current density in 0.01 M $RuCl_3$ + 0.1 M HCl electrolyte (area of the electrode = 0.6 cm^2).

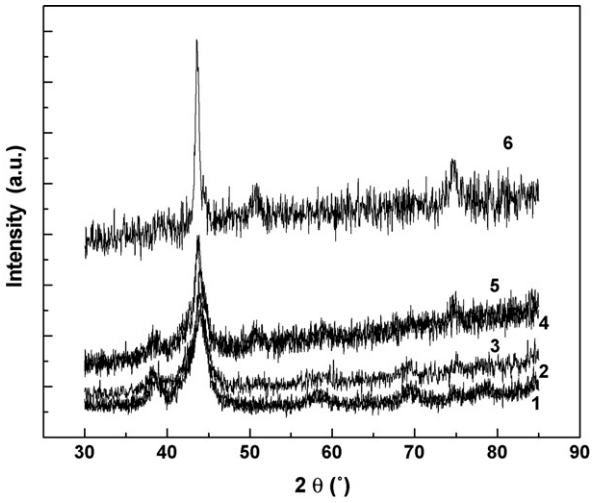

Fig. 3. X-ray diffraction patterns of RuO_2/SS deposited at a current density of (1) 15, (2) 20, (3) 25, (4) 30 and (5) 35 mA cm^{-2} to a specific mass of about 1.5 mg of RuO_2 cm^{-2}. Diffraction pattern (6) is for bare SS substrate.

where i_0 is the exchange-current density, β is the transfer coefficient and other symbols have their usual meanings. The Tafel slope obtained is about 117 mV $decade^{-1}$. These results suggest that the anodic deposition of RuO_2 occurs by oxidation of Ru^{3+} (reaction (1)) as an electron-transfer controlled reaction in $RuCl_3$ solution at a concentration as low as 0.01 M. The mechanism of oxidation of Ru^{3+} to RuO_2 (reaction (1)) is likely to consist of the following steps:

$$Ru^{3+} \rightarrow Ru^{4+} + e^- \quad (3)$$

$$Ru^{4+} + 2H_2O \rightarrow RuO_2 + 4H^+ \quad (4)$$

The increasing current at about 1.2 V (Fig. 1) is due to commencement of oxygen evolution reaction (OER, reaction (5)).

$$2H_2O \rightarrow O_2 + 4H^+ + 4e^- \quad (5)$$

It may be noted that the current density values used for electrodeposition of RuO_2 on SS substrates fall in the transition between the Tafel regime of reaction (1) and reaction (5). Under these conditions, both reactions (1) and (5) occur simultaneously.

Subsequent to recording the Tafel measurements on Pt anode, RuO_2 was deposited on SS substrate for further experiments. Cyclic voltammograms for SS substrate recorded in 0.01 M $RuCl_3$ + 0.1 M HCl did not indicate oxidation of the substrate,

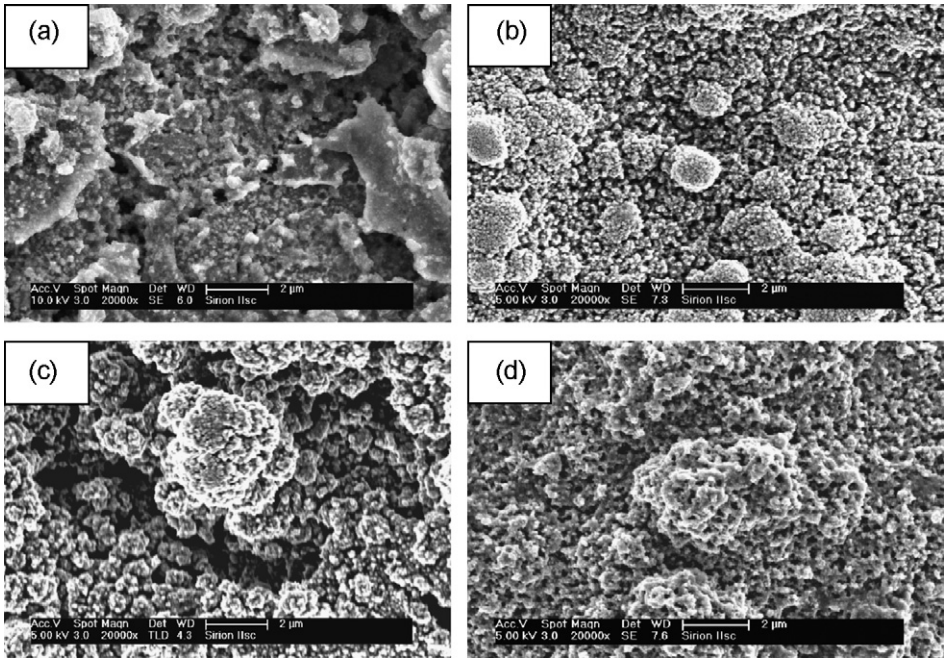

Fig. 4. Scanning electron micrograph of RuO_2/SS electrodes prepared at a current density of (a) 15, (b) 25, (c) 30 and (d) 35 mA cm^{-2}.

and voltammograms were similar to the data obtained using Pt substrate. Thus, stability of SS substrate in the electrolyte during deposition of RuO_2 was ensured. Several RuO_2/SS electrodes were prepared by varying deposition c.d. in the range of 15–35 mA cm^{-2} in 0.01 $RuCl_3$ + 0.1 M HCl electrolyte. As this range of c.d. corresponds to the transition region between reactions (1) and (5) (Fig. 1), the RuO_2 deposition occurs on SS with simultaneous oxygen evolution. It was attempted to calculate the charge consumed by each of these two reactions out of the charge passed. The galvanostatic charge (Q_t) was measured from the experiment. After the deposition, the RuO_2/SS electrode was washed, dried and weighed to reproducible weight. Using the mass and the Faraday's law, the charge (Q_d) required for the deposition of RuO_2 from Ru^{+3} was calculated. The difference in charges ($Q_t - Q_d$) was considered to be the charge consumed for OER. The variation of relative charges with the c.d. is shown in Fig. 2. It is interesting to note that the major part (98.5–99.5%) of charge is consumed for the OER. There is a slight decrease in the charge consumed by OER with an increase in c.d. However, the rate of OER is higher at higher c.d. As it is discussed below, capacitance properties of RuO_2/SS electrodes prepared at high c.d. with a high OER rate are superior to the electrodes prepared at lower c.d.

The XRD patterns of RuO_2/SS electrodes are shown in Fig. 3. The peak at $2\theta = 44^\circ$ corresponds to the SS substrate. The rest of the patterns with minor peaks indicate that RuO_2 deposited at all c.d. is in an amorphous state. The small peaks corresponding to RuO_2 are broad, suggesting fine particle-size. The surface morphology of RuO_2/SS electrodes was examined by scanning electron microscope and the micrographs are shown in Fig. 4. The RuO_2 films deposited at 15 mA cm^{-2} appear to have flake-like morphology (Fig. 4(a)). When the c.d. is 25 mA cm^{-2}, the deposit develops porosity (Fig. 4(b)). With an increase in deposition c.d., the porosity increases as reflected in Fig. 4(c) and (d) for RuO_2 deposited at 30 and 35 mA cm^{-2}, respectively. The increase in porosity at high c.d. of anodic deposition is due to increased oxygen evolution rate. When oxidation of H_2O to O_2 (reaction (2)) occurs, simultaneously with RuO_2 deposition, a fraction of the electrode surface is covered with O_2 or intermediates such as O_{ads}, OH_{ads}, etc. These adsorbed species do not allow the oxidation of Ru^{3+} to take place at these sites, but RuO_2 forms at the neighbouring sites, which are free from the adsorbed species. The sites covered with adsorbed species would be available for RuO_2 deposition after the species get desorbed. Hence the deposition of RuO_2 occurs now on the sites where it did not occur earlier. Similarly, the adsorbed sites keep changing on the electrode surface. Due to continuous change in the sites of the simultaneous oxidation of Ru^{3+} and H_2O during electrolysis on the SS substrate, porosity develops on RuO_2 deposit. The porosity of RuO_2 increases with c.d. used for electrolysis because of faster changing of the adsorption and deposition sites.

Since RuO_2 was prepared as a thin layer by anodic oxidation on SS substrate, XPS was used to identify the presence of RuO_2. XPS core level spectra of Ru $3P_{3/2}$ and O 1S for RuO_2 are shown in Fig. 5(a) and (b), respectively. These XPS data are similar to

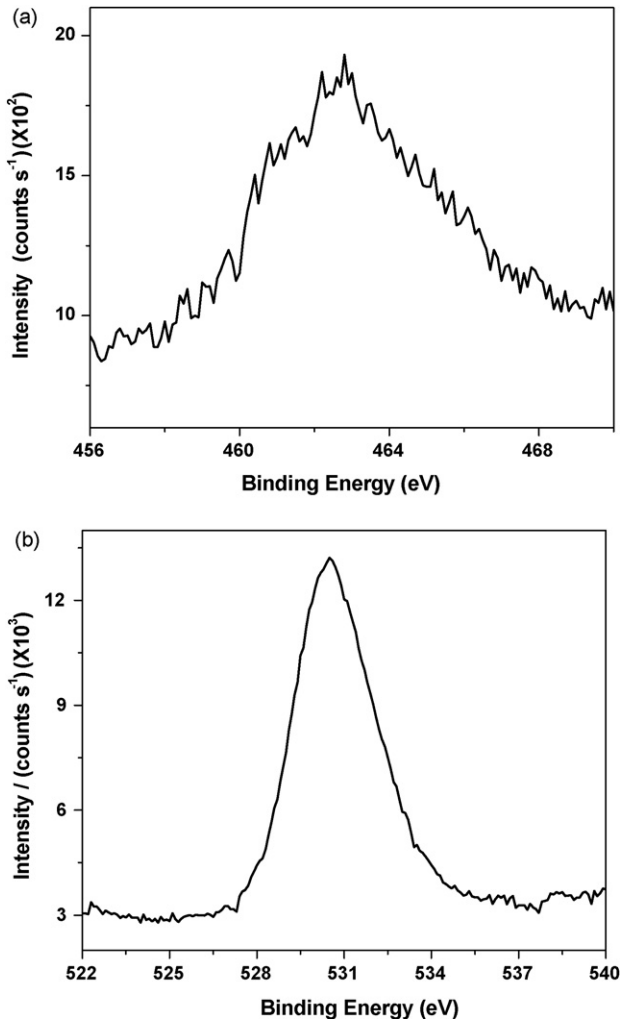

Fig. 5. XPS spectra of (a) Ru $3P_{3/2}$ and (b) O 1s for the anodically deposited RuO_2/SS electrode.

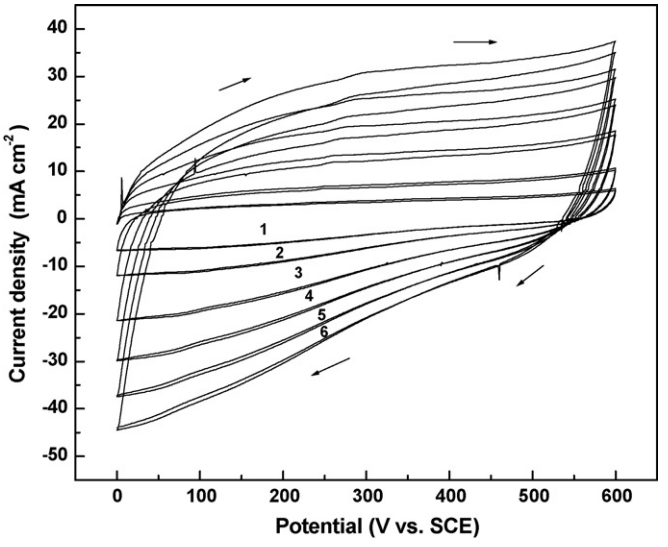

Fig. 6. Cyclic voltammograms of RuO_2/SS electrode deposited at 35 mA cm^{-2} in 0.01 M $RuCl_3$ + 0.1 M HCl. Voltammograms were recorded in 0.5 M H_2SO_4 at a sweep rate of (1) 5, (2) 10, (3) 20, (4) 30, (5) 40 and (6) 50 mV s^{-1}. Mass of RuO_2: 1.5 mg cm^{-2}.

the data reported by Chang and Hu for RuO_2 synthesized by a chemical route [12]. The Ru $3P_{3/2}$ spectrum was centered at binding energy (BE) of 464 eV, and it was decomposed into three Gaussian peaks with their BE centered at 462.2, 463.8 and 466.9 eV, respectively [12]. The 462.2 eV peak was assigned to anhydrous RuO_2, the peak at 463.8 eV was to hydrous RuO_2 and the peak 466.9 eV was to Ru(VI) species. The Ru(VI) species was assumed to be RuO_3. The main component was hydrous RuO_2. The O 1s spectrum was resolved into three constituents, which are bridged oxygen (Ru–O–Ru) with BE at 530 eV, the hydroxide (Ru–O–H) with BE at 531.2 eV, and water molecule (H–O–H) 533.3 eV, respectively [12]. The main O species was Ru–O–H. These results confirmed that the synthesized sample from $RuCl_3$ was hydrated RuO_2. As the XPS data shown in Fig. 5 are almost identical to the data reported in Ref. [12], it is anticipated that RuO_2 prepared by anodic oxidation of $RuCl_3$ is also present in the hydrated form.

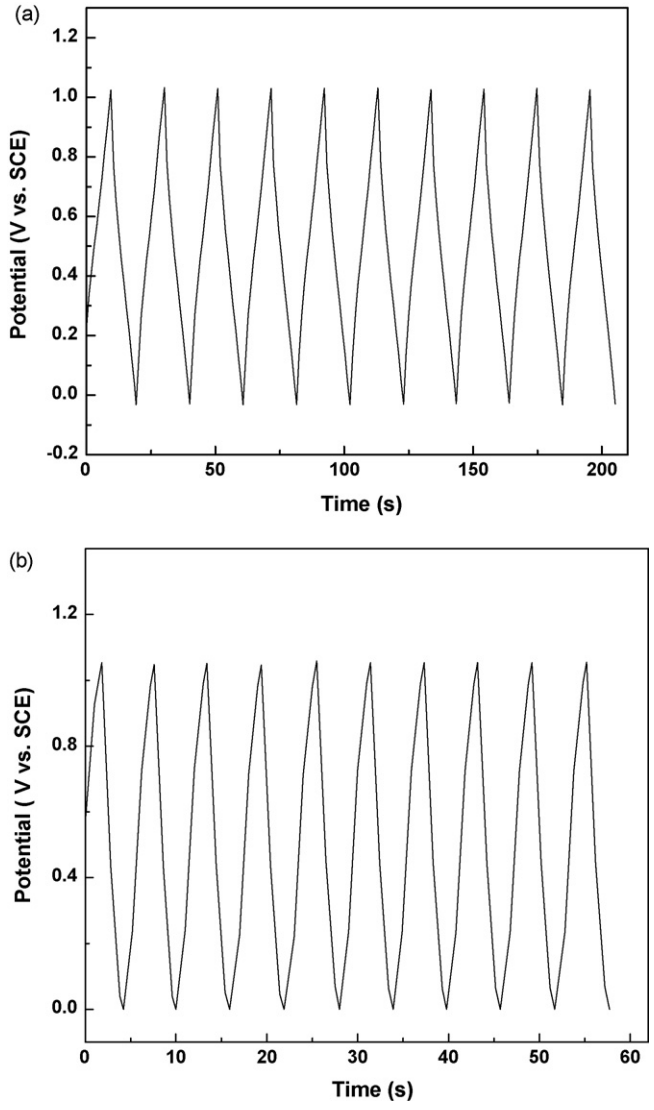

Fig. 7. Charge–discharge cycle data of RuO_2/SS electrode prepared in (a) 0.01 M $RuCl_3$ + 0.1 M HCl and (b) 0.1 M $RuCl_3$ + 0.1 M HCl at 35 mA cm^{-2}. The current density used for cycling was 20 mA cm^{-2}. Mass of RuO_2: 1.5 mg cm^{-2}.

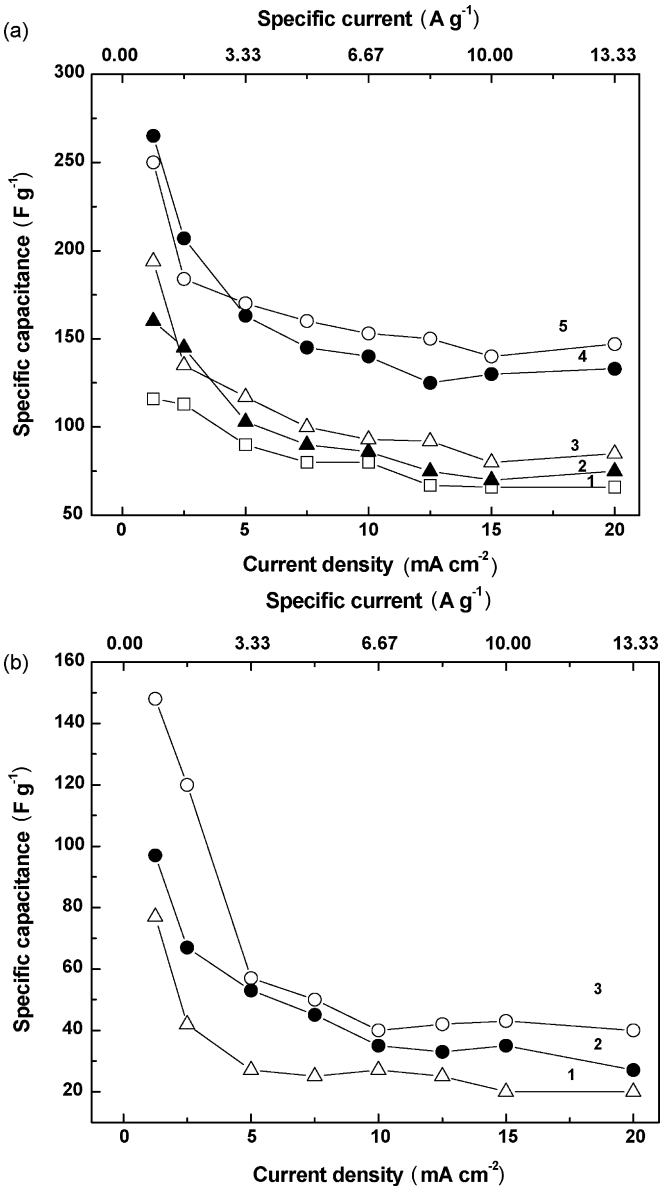

Fig. 8. Specific capacitance versus charge–discharge current density for RuO_2/SS electrodes prepared in (a) 0.01 M $RuCl_3$ + 0.1 M HCl electrolyte at (1) 15, (2) 20, (3) 25, (4) 30 and (5) 35 mA cm^{-2} and (b) 0.1 M $RuCl_3$ + 0.1 M HCl electrolyte at (1) 25, (2) 30 and (3) 35 mA cm^{-2}. Mass of RuO_2: 1.5 mg cm^{-2}.

RuO_2/SS electrodes were subjected to cyclic voltammetry in 0.5 M H_2SO_4 and they were found to exhibit capacitance behaviour. Voltammograms of RuO_2/SS electrode prepared at 35 mA cm^{-2} in 0.01 M $RuCl_3$ + 0.1 M HCl electrolyte are typically shown in Fig. 6. No sharp current peaks are present and the voltammogram is close to rectangular shape. Similar voltammograms were reported for cathodically deposited RuO_2 films on Ti substrate [14]. As expected, there is an increase in current of the voltammograms with an increase in sweep rate (Fig. 6).

Values of specific capacitance of the RuO_2/SS electrodes were measured from galvanostatic charge–discharge cycling. Typical charge–discharge curves of electrodes prepared at 35 mA cm^{-2} in 0.01 M $RuCl_3$ + 0.1 M HCl and also in 0.1 M $RuCl_3$ + 0.1 M HCl electrolytes are shown in Fig. 7. The c.d.

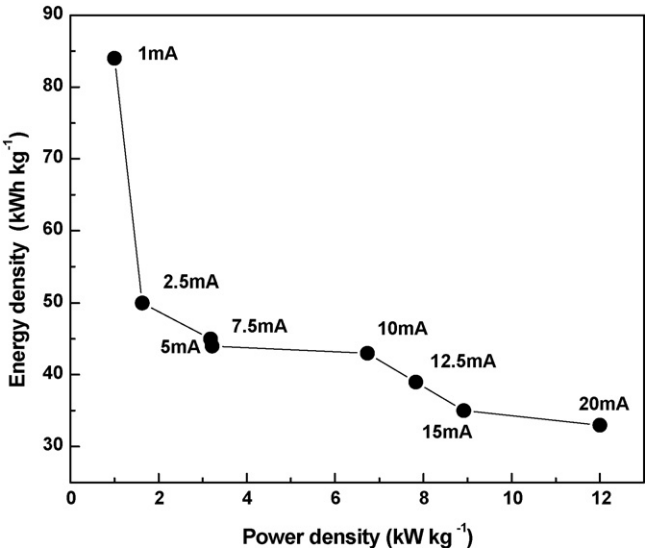

Fig. 9. Energy density versus power density of RuO_2/SS electrode prepared in 0.01 M $RuCl_3$ + 0.1 M HCl electrolyte at 35 mA cm^{-2}.

used for charge and discharge cycling was 20 mA cm^{-2} with a specific current of 13.33 A g^{-1}. There is a linear variation of potential during charge and discharge processes (Fig. 7(a) and (b)). The specific capacitance of the electrode was calculated using the following equation.

$$SC = \frac{It}{Vm} \quad (5)$$

where I is the current, t is the discharge time, V is the potential range and m is the mass of RuO_2. The discharge capacitance obtained from Fig. 7(a) is 276 F g^{-1}, and the Faradaic efficiency of charge–discharge cycling is 96%. Thus, RuO_2/SS electrodes prepared by galvanostatic deposition possess good capacitance behaviour as evidence by both cyclic voltammetry (Fig. 6) and galvanostatic charge–discharge cycling (Fig. 7).

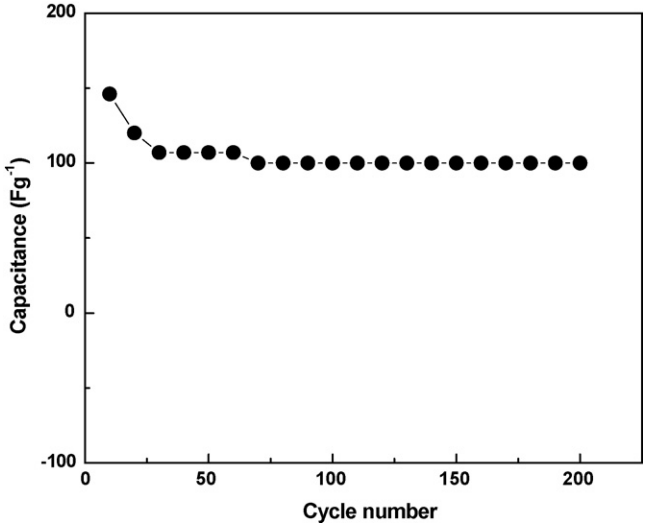

Fig. 10. Cycle-life data of RuO_2/SS electrode prepared in 0.01 M $RuCl_3$ + 0.1 M HCl electrolyte at 35 mA cm^{-2}.

RuO_2/SS electrodes were prepared in 0.01 M $RuCl_3$ + 0.1 M HCl and also 0.1 M $RuCl_3$ + 0.1 M HCl electrolytes at different c.d. values. They were subjected to charge–discharge cycling in 0.5 M H_2SO_4 using different c.d. Specific capacitance data are plotted as a function of charge–discharge c.d. and shown in Fig. 8. Several important inclusions can be drawn from these data. A comparison of Fig. 8(a) and (b) suggests that RuO_2 deposited in 0.01 M $RuCl_3$ yields higher SC than the deposits prepared in 0.1 M $RuCl_3$. When $RuCl_3$ concentration is low, oxygen evolution is more vigorous, therefore, the deposited RuO_2 films possess greater porosity than the deposits prepared in an electrolyte with higher concentration of $RuCl_3$. Greater porosity facilitates higher utilization efficiency of the electroactive material and also allows higher c.d. of charge–discharge cycling. In both 0.01 M and 0.1 M $RuCl_3$ electrolytes, RuO_2 electrodes prepared at higher deposition current densities yield higher SC. Again, this feature is also due to increased oxygen evolution rate at higher deposition current densities, there by causing greater porosity. For all electrodes, there is a decrease in SC with an increase in charge–discharge c.d. In literature, the c.d. values used for charge–discharge cycling of RuO_2 electrodes are very low. For instance, Hu and Huang [15] deposited RuO_2 on Ti substrate by cyclic voltammetry and charge–discharge cycling of the electrodes was studied at a c.d. of 100 μA cm^{-2}. Specific capacitance of 101.4 F g^{-1} was obtained. It is interesting to note that RuO_2/SS electrodes prepared in the present study allow charge–discharge current densities as high as 20 mA cm^{-2} (or, 13.33 A g^{-1}). Specific capacitance value obtained at this high current density is about 150 F g^{-1}, which is also a reasonably high value. High values of c.d. are advantageous for using the RuO_2/SS electrodes for high power applications. Variation of energy density with power density for a RuO_2/SS electrode prepared in 0.01 M $RuCl_3$ + 0.1 M HCl electrolyte at 35 mA cm^{-2} is shown in Fig. 9. It is seen that power density values are as high as 12 kW kg^{-1}. An electrode was subjected to a large number of charge–discharge cycles and SC versus cycle number is presented in Fig. 10. Although there is a decrease in SC during the initial cycling, a stable SC of about 100 F g^{-1} is obtained over 200 cycles.

4. Conclusions

Anodic deposition of RuO_2 on SS was successfully carried out for supercapacitor studies. As the deposition occurs during simultaneous oxygen evolution, the RuO_2 films acquire porosity. The porous RuO_2/SS electrodes allow high values of current for charge–discharge cycling.

Acknowledgement

Authors thank Prof. M.S. Hegde and Mr. Tinku for recoding XPS.

References

[1] S. Trasatti, G. Lodi, in: S. Trasatti (Ed.), Condutive Metal Oxides, vol. A, Elsevier, Amsterdam, 1980, p. 338.

[2] D. Galizzioli, F. Tantardini, S. Trasatti, J. Appl. Electrochem. 4 (1974) 57.
[3] S. Trasatti, G. Buzzanca, J. Electroanal. Chem. 29 (1971) 1.
[4] S.H. Jordanov, H.A. Kozlowska, B.E. Conway, J. Electroanal. Chem. 60 (1975) 359.
[5] S.H. Jordanov, H.A. Kozlowska, B.E. Conway, J. Phys. Chem. 81 (1977) 2271.
[6] B.E. Conway, Electrochemical Supercapacitors, Kluwer Academic/Plenum Publishers, NY, 1999, p. 259.
[7] S.H. Jordanov, H.A. Kozlowska, B.E. Conway, J. Electrochem. Soc. 125 (1978) 1471.
[8] J.P. Zheng, T.R. Jow, J. Electrochem. Soc. 142 (1995) L6.
[9] J.P. Zheng, P.J. Cygan, T.R. Jow, J. Electrochem. Soc. 142 (1995) 2699.
[10] N.L. Wu, S.L. Kuo, M.H. Lee, J. Power Sources 194 (2002) 62.
[11] Y.G. Wang, X.G. Zhang, Electrochim. Acta 49 (2004) 1957.
[12] K.H. Chang, C.C. Hu, J. Electrochem. Soc. 151 (2004) A958.
[13] I. Zhitomirsky, L. Gal-Or, Mater. Lett. 31 (1997) 155.
[14] B.O. Park, C.D. Lokhande, H.S. Park, K.D. Jung, O.S. Joo, J. Mater. Sci. 39 (2004) 4313.
[15] C.C. Hu, Y.H. Huang, J. Electrochem. Soc. 146 (1999) 2465.
[16] D.P. Anderson, L.F. Warren, J. Electrochem. Soc. 131 (1984) 347.
[17] C.C. Hu, M.J. Liu, K.H. Chang, J. Power Sources 163 (2007) 1126.